Supporting Information for

Subtle Structural Modification of Thiophene-fused Benzotriazole Unit to Simultaneously Improving J_{SC} and V_{OC} for OSCs

Yajing Zhang[a], Cheng Zhong[a], Guilong Cai[d], Yawen Li[c], Jiayu Wang[b], Heng Lu[b], Boyu Jia[b], Xinhui Lu[d], Yuze Lin[c*], Xiaowei Zhan[b*] and Xingguo Chen[a*]

[a]Hubei Key Laboratory on Organic and Polymeric Opto-electronic Materials, College of Chemistry and Molecular Sciences, Wuhan University, Wuhan 430072, China. E-mail: xgchen@whu.edu.cn.

[b]School of Materials Science and Engineering, Peking University, Beijing 100871, China. E-mail: xwzhan@pku.edu.cn.

[c]Beijing National Laboratory for Molecular Sciences, CAS Key Laboratory of Organic Solids, Institute of Chemistry, Chinese Academy of Sciences, Beijing 100190, China. E-mail: linyz@iccas.ac.cn.

[d]Department of Physics, Chinese University of Hong Kong, New Territories 999077, Hong Kong, China.

Instruments and measurements

^{1}H-NMR and ^{13}C-NMR were measured on a Bruker AVANCE III HD 400MHz. The thermogravimetric analysis (TGA) was performed on TA thermal analyzer (model Q600 SDT) under a nitrogen flow at a heating rate of 10 ^{o}C min^{-1}. The molecular weight and dispersion of the polymer were measured by gel permeation chromatography (GPC) (PL-GPC220 of Polymer Laboratories Ltd). The thickness of active layer was measured on a Bruker DektakXT profilometer. Elemental analyses were carried out on a 73 CARLOERBA-1106 microelemental analyzer. The electronic energy levels were measured by electrochemical cyclic voltammetry (CV) and refer to the Leeuw empirical formula: HOMO = -(E_{onset}^{ox} + 4.8 − 0.48); LUMO = -(E_{onset}^{red} + 4.8 − 0.48). The CV was conducted on a CHI voltammetric analyzer with glassy carbon disk, Pt wire and Ag/Ag$^+$ electrode as working electrode, counter electrode and reference electrode respectively in a 0.1 mol L^{-1} tetrabutylammonium hexafluorophosphate (Bu_4NPF_6) acetonitrile solution. The UV-vis absorption spectra of the materials were measured by a Varian Cary 5000 UV-vis-NIR spectrophotometer. The photoluminescence spectra (PL) were determined with Edinburgh FLS980 spectrometer. Atomic force microscope (AFM)

images were measured on Multimode 8 scanning probe microscopy (Bruker Daltonics Inc., United States) in the tapping mode to investigate the nanoscale morphology of the blends. The transmission electron microscopy (TEM) characterization was carried out on a JEM-2100 transmission electron microscope operated at 200 kV. The GIWAXS measurements are conducted at 14B1 and 19U2 beamline at Shanghai Synchrotron Radiation Facility, Shanghai, China with 10 keV primary beam, 0.15° incidence angle and Mar 225 CCD and Pilatus 1M-F detector, respectively. The samples for GIWAXS measurements are fabricated on silicon substrates using the same recipe for the devices.

Fabrication and characterization of organic solar cells

Organic solar cells were fabricated with the structure: ITO / PEDOT:PSS / active layer / F3N / Ag. The indium tin oxide (ITO) glass (sheet resistance = 10 Ω sq^{-1}) was pre-cleaned in an ultrasonic bath of deionized water, acetone and isopropanol. PEDOT:PSS layer (*ca.*30 nm) was spin-coated onto the ITO glass, and baked at 150 °C for 15 min. A chloroform solution of active layer (16 mg mL^{-1} in total) was spin-coated on PEDOT:PSS layer to form a photoactive layer. The thicknesses of active layers were an average of 100 nm as measured by a profilometer. The Ag (70 nm for opaque devices) was successively evaporated onto the surface of the photoactive layer under vacuum (*ca.*10^{-5}Pa). The active area of the device was 4.0 mm^2, defined under an optical microscope. The *J-V* curve was measured using a computer-controlled B2912A Precision Source/Measure Unit (Agilent Technologies). An XES-70S1 (SAN-EI Electric Co., Ltd.) solar simulator (AAA grade, 70 × 70 mm^2 photobeam size) coupled with AM 1.5G solar spectrum filters was used as the light source, and the optical power at the sample was 100 mW cm^{-2}. A 2 × 2 cm^2 monocrystalline silicon reference cell (SRC-1000-TC-QZ) was purchased from VLSI Standards Inc. The EQE spectra were measured using a Solar Cell Spectral Response Measurement System QE-R3011 (Enlitech Co., Ltd.). The light intensity at each wavelength was calibrated using a standard single crystal Si photovoltaic cell.

Mobility measurements

Hole-only and electron-only diodes were fabricated using the architectures: ITO / PEDOT:PSS / active layer /Au for holes and ITO / ZnO / active layer / Al for electrons. Mobilities were extracted by

fitting the current density–voltage curves using space-charge-limited current (SCLC) method. The *J-V* curves of the devices were plotted as $\ln(Jd^3/V^2)$ versus $(V/d)^{0.5}$ using the equation $\ln(Jd^3/V^2) \cong 0.89(1/E_0)^{0.5}(V/d)^{0.5} + \ln(9\varepsilon_0\varepsilon_r\mu/8)$, where J is the current density, E_0 is characteristic field, d is the film thickness of active layer, μ is the hole or electron mobility, ε_r is the relative dielectric constant of the transport medium, ε_0 is the permittivity of free space (8.85×10^{-12} F m^{-1}), $V = V_{appl} - V_{bi}$, where V_{appl} is the applied voltage to the device, and V_{bi} is the built-in voltage due to the difference in work function of the two electrodes (for hole-only diodes, V_{bi} is 0.2 V; for electron-only diodes, V_{bi} is 0 V).

Voltage loss calculation

According to detailed balance theory, V_{OC} of a BHJ solar cell is determined by E_{CT}, radiative, and non-radiative recombination losses of charge carriers:

$$V_{loss} = E_g/q - V_{OC} = (E_g - E_{CT})/q + k_B T \ln(EQE_{EL}^{-1})/q + \Delta V_{rad} = \Delta E_{CT}/q + \Delta V_{nonrad} + \Delta V_{rad} \quad \textbf{(S1)}$$

q is the elementary charge, E_g is the bandgap of the blend film, k_B is the Boltzmann constant, T is the absolute temperature in Kelvin, EQE_{EL} is the EQE of EL, ΔV_{rad} is the radiative recombination voltage loss, ΔE_{CT} is defined as the offset between E_g and E_{CT}, ΔV_{nonrad} represents the non-radiative recombination voltage loss.

Syntheses of compounds

Synthesis of compound 2. The compound 1(1.5 g, 3.59 mmol) was added to the flask, which was purged by Ar_2 for three times. Then, anhydrous THF (50 mL) was added to it and the mixture was stirred for 30 mins at - 78 °C. Then n-butyl lithium (4.308 mmol, 1.72 mL) solution was slowly added and stirred for 30 minutes. Then, NFSI (3.40 g, 10.77 mmol) was added, heated to 50 °C for 8 h, After the reaction, the mixture was evaporated to afford the crude product, which was purified by column chromatography to give the product 2 as colorless oily (891 mg, 57 % yield). ^{1}H NMR (400 MHz, $CDCl_3$, δ ppm) 8.14 (s, 1H), 8.13 (s, 1H), 4.67 (d, J = 7.1 Hz, 2H), 2.34 – 2.24 (m, 1H), 1.45 – 1.14 (m, 24H), 0.89-0.80 (m, 6H). ^{13}C NMR (101 MHz, $CDCl_3$, δ ppm) 143.33, 143.02, 142.64, 127.23, 127.03, 125.42, 112.15, 108.27, 60.87, 39.33, 31.81, 31.37, 29.62, 29.27, 26.20, 22.65, 14.11. EI-MS:Calcd.For$[C_{24}H_{35}F_2N_3S]^+$: 435.25; Found: 435.50.

Synthesis of compound 3. The compound 2 (0.5 g, 1.15 mmol) was added to inround-bottom flask (250 mL), add chloroform (50 mL) and acetic acid (5 mL), then add liquid bromine(1 mL), heat up to 50 °C and stir for 12 h. After the reaction, the mixture was washed with sodium bisulfite and sodium bicarbonate, then evaporated to afford the crude product, which was purified by column chromatography to give the product 3 as colorless oily (375 mg, 55% yield). ^{1}H NMR (400 MHz, $CDCl_3$, δ ppm) 4.65 (d, *J* = 7.2 Hz, 2H), 2.31 (d, *J* = 5.2 Hz, 1H), 1.43 – 1.11 (m, 24H), 0.88-0.94 (m, 6H). ^{13}C NMR (101 MHz, $CDCl_3$, δ ppm) 143.97, 143.37, 132.32, 130.90, 111.17,110.82, 109.17, 104.37, 61.38, 39.10, 31.80, 31.08, 29.78, 29.57, 29.18, 26.00, 22.67, 14.16. EI-MS: Calcd.For$[C_{24}H_{33}Br_2F_2N_3S]^+$: 593.07; Found: 593.43.

Synthesis of compound 4. The compound 3 (0.4 g, 0.674 mmol), 2-trimethyl tin thiophene (578.5 mg, 1.55 mmol), catalyst $Pd(PPh_3)_4$ (3 mg) were added to the flask, which was purged by Ar_2 for three times. Then, anhydrous toluene (15 mL) was added to it and the mixture was stirred for 12 h at 110 °C After the reaction, the mixture was evaporated to afford the crude product, which was purified by column chromatography to give the product 4 as yellow solid (303 mg, 75 % yield). ^{1}H NMR (400 MHz, $CDCl_3$, δ ppm): 8.03 (dd, *J* = 3.7, 1.1 Hz, 1H), 7.61 (dd, *J* = 5.1, 1.1 Hz, 1H), 7.58 (dd, *J* = 5.1, 1.1 Hz, 1H), 7.39 (dd, *J* = 5.8, 2.3 Hz, 1H), 7.30 (dd, *J* = 5.1, 3.7 Hz, 1H), 7.22 (dd, *J* = 5.1, 3.6 Hz, 1H), 4.72 (t, *J* = 6.6 Hz, 2H), 2.32 (dd, *J* = 11.7, 5.8 Hz, 1H), 1.42 – 1.19 (m, 24H), 0.90 (m, 6H). ^{13}C NMR (101 MHz, $CDCl_3$, δ ppm): 147.75, 143.46, 140.80, 136.23, 135.79, 134.05, 133.47, 129.71, 129.22, 127.94, 127.42, 126.79, 124.02, 123.43, 118.98, 117.37, 60.53, 39.15, 31.88, 31.40, 29.93, 29.59, 29.35, 28.32, 26.84, 26.19, 22.71, 17.32, 14.17, 13.66. EI-MS: Calcd.For$[C_{24}H_{35}F_2N_3S]^+$: 599.23; Found: 599.81 .

Synthesis of monomer M2. To the compound 4 (0.5 g, 0.833 mmol) in chloroform (50 mL), NBS (311 mg, 1.75 mmol) was added and mixture was stirred for 8 h at room temperature. After the reaction, the mixture was evaporated to afford the crude product, which was purified by column chromatography to give a monomer M2 as yellow solid (600 mg, 95% yield). ^{1}H NMR (400 MHz, $CDCl_3$, δ ppm): 7.70 (d, *J* = 4.0 Hz, 1H), 7.23 (d, *J* = 4.0 Hz, 1H), 7.15 (d, *J* = 3.9 Hz, 1H), 7.13 – 7.09 (m, 1H), 4.72 (d, *J* = 6.7 Hz, 2H), 2.29 (d, *J* = 6.2 Hz, 1H), 1.44 – 1.14 (m, 24H), 0.97 – 0.72 (m, 6H). ^{13}C NMR (101 MHz, $CDCl_3$, δ ppm): 147.71, 143.06, 140.43, 137.32, 135.91, 135.43, 130.41, 130.04, 129.77, 129.25, 123.82, 123.10, 118.26, 116.49, 115.95, 114.72, 60.49, 39.22, 31.89, 31.40, 29.96, 29.62, 29.36, 26.18,

22.71, 14.17. HRMS: Calcd.For $[C_{32}H_{37}Br_2F_2N_3S_3]^+$: 757.0464; Found:757.0461.

Preparation of PffBTAZT-fBDT: Monomer M2 (90.0 mg, 0.119 mmol), monomer M3 (111.7 mg, 0.119 mmol) and $Pd(PPh_3)_4$ (8 mg) were added to a Schlenk flask, which was purged by Ar_2 for three times. And then, anhydrous toluene (10 mL) was added to the flask. The mixture was stirred for 48 h at 110°C. After cooling, the mixture was precipitated into CH_3OH. The unpurified polymer was put into Soxhlet extraction and extracted with methanol, acetone, hexane and $CHCl_3$, respectively. The resulted chloroform fraction was re-precipitated in methanol. Then the precipitate was collected to give PffBTAZT-fBDT as dark blue solid. GPC: M_n =31.7 kDa, PDI=1.91. Anal. Calcd for $C_{66}H_{75}F_4N_3S_7$ (%):C 65.47, H 6.24, N 3.47. Found: C 65.32, H 6.19, N 3.62.

Table S1. The parameters of **PfBTAZT-fBDT** or **PffBTAZT-fBDT:Y**6 based devices with annealing conditions at 130 °C/2 min and different D/A ratios.

Devices	D:A (w/w)	V_{OC} (V)	J_{SC} (mA/cm^2)	FF (%)	PCE (%)
PfBTAZT-fBDT:Y6	1:1	0.616	21.04	43.90	5.69
	1:1.25	0.601	18.86	44.38	5.03
	1.5:1	0.638	23.89	47.79	7.28
PffBTAZT-fBDT:Y6	1:1	0.819	26.57	62.92	13.68
	1:1.25	0.814	24.96	64.35	13.08
	1.25:1	0.824	25.71	63.45	13.45

Table S2. The parameters of **PfBTAZT-fBDT** or **PffBTAZT-fBDT:Y6** based devices with optimized D/A ratios, annealing temperature and different solvent additive.

Devices	Additive (v/v)	Temperature (°C)	V_{OC} (V)	J_{sc} (mA/cm^2)	FF (%)	PCE (%)
PfBTAZT-fBDT:Y6[a]	w/o	RT	0.663	20.40	42.44	5.74
	0.25% CN	140	0.662	20.23	47.40	6.35
	0.5% CN	130	0.661	21.41	48.83	6.91
	0.75% CN	140	0.644	20.18	41.14	5.35
	0.5% DPE	130	0.617	21.36	46.45	6.13
PffBTAZT-fBDT:Y6[b]	w/o	RT	0.852	24.27	61.13	12.64
	0.25%CN	140	0.824	25.86	66.39	14.15
	0.25% DPE	130	0.815	26.35	66.06	14.18
	0.5% DPE	130	0.802	23.77	67.63	12.90
	0.15% DPE	130	0.820	23.25	68.46	13.06

[a]D/A radio of 1.5:1; [b]D/A radio of 1:1.

Table S3. Carrier transport properties of optimized polymer:Y6 blended films.

Devices	μ_h (cm^2 V^{-1} s^{-1})	μ_e (cm^2 V^{-1} s^{-1})	μ_h/μ_e
PfBTAZT-fBDT:Y6	8.27×10^{-5}	3.72×10^{-5}	2.23
PffBTAZT-fBDT:Y6	1.67×10^{-4}	9.14×10^{-5}	1.82

Table S4. The GPC of PfBTAZT-fBDT and PffBTAZT-fBDT

SampleName	M_n	M_w	M_P	PDI	Area (%)
PfBTAZT-fBDT	85117	214466	191033	2.52	100.00
PffBTAZT-fBDT	31691	60520	46157	1.91	85.00

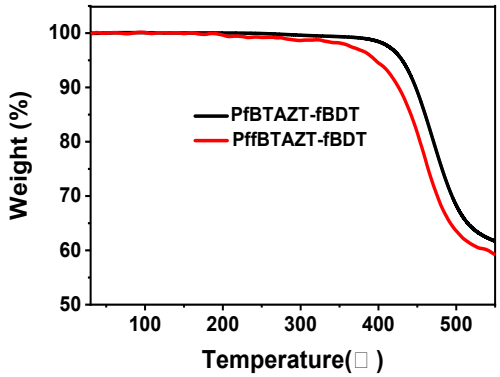

Fig. S1 The TGA curves of **PfBTAZT-fBDT** and **PffBTAZT-fBDT**.

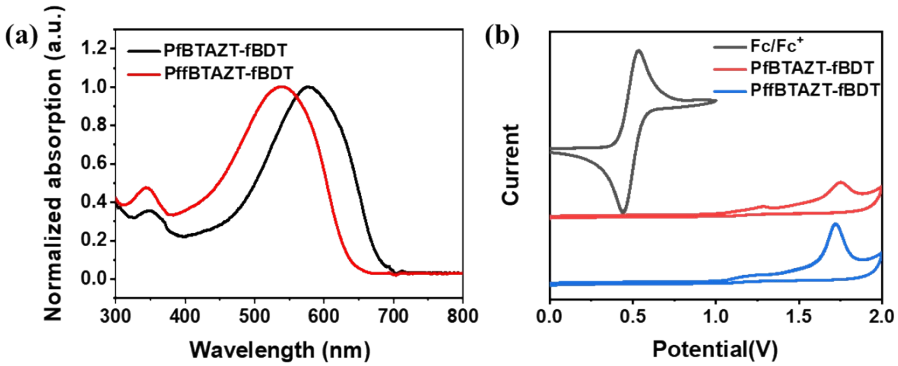

Fig. S2 (a) Normalized absorption spectra of polymer donors in solution; (b) The CV curves of **PfBTAZT-fBDT** and **PffBTAZT-fBDT** in CH3CN/0.1 M Bu4NPF6 at 100 mV s^{-1}.

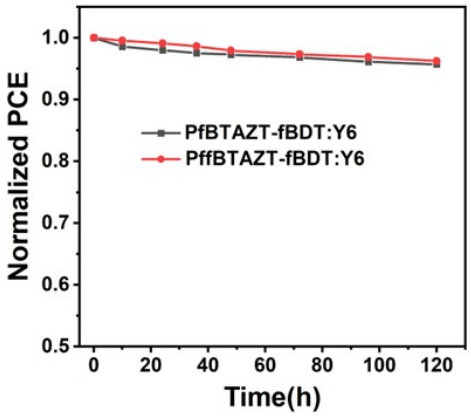

Fig. S3 Normalized PCEs of the storage stability under a nitrogen atmosphere

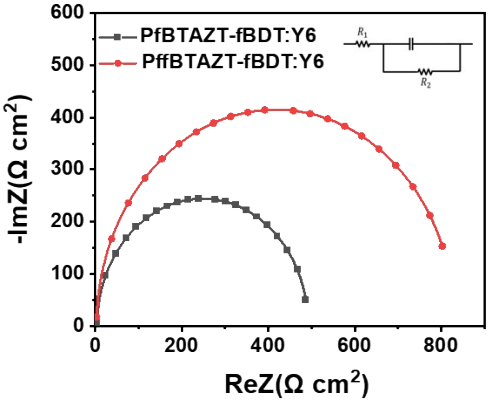

Fig. S4 Nyquist plots of the devices (the inset is the equivalent circuit model)

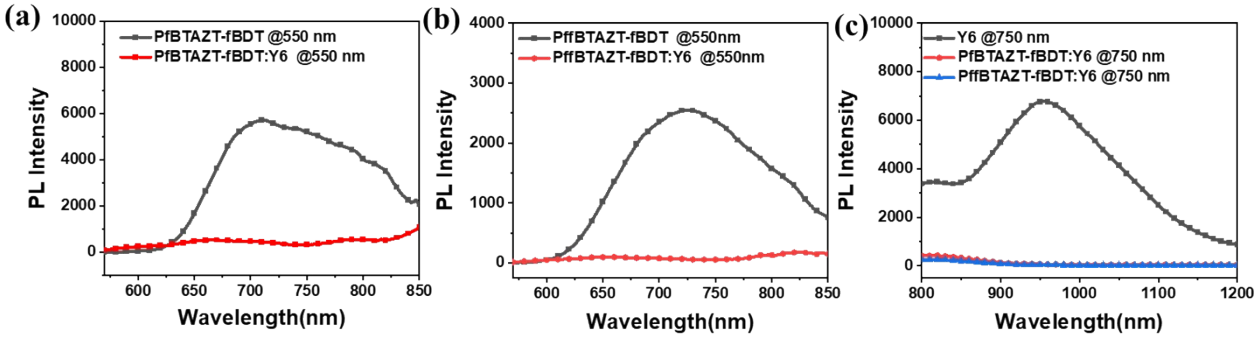

Fig. S5 Photoluminescence spectra of the polymers (excited at 550 nm) and Y6 (excited at 750 nm) films as well as the polymer:Y6 blend films of (1:1, w/w) (excited at 550 and 750 nm, respectively).

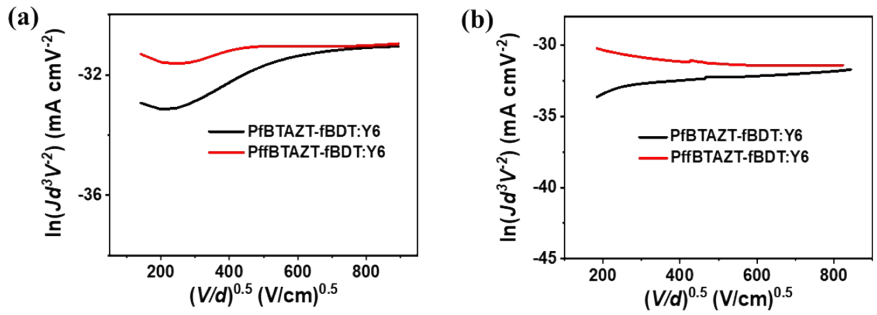

Fig. S6 $\ln(Jd^3/V^2)$ vs $(V/d)^{0.5}$ plot for (a) the hole mobility and (b) electron mobility measurements based on optimized **PfBTAZT-fBDT: Y6** and **PffBTAZT-fBDT:Y6** blended films.

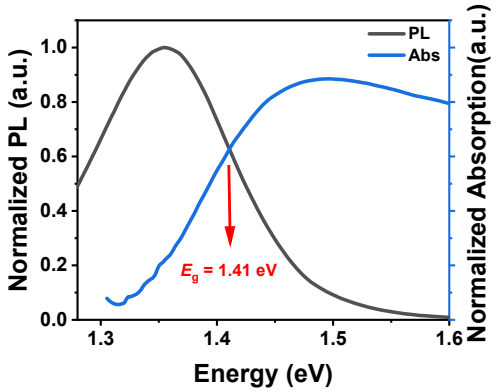

Fig. S7 Normalized PL and absorption (abs) spectra of the pure Y6 film.

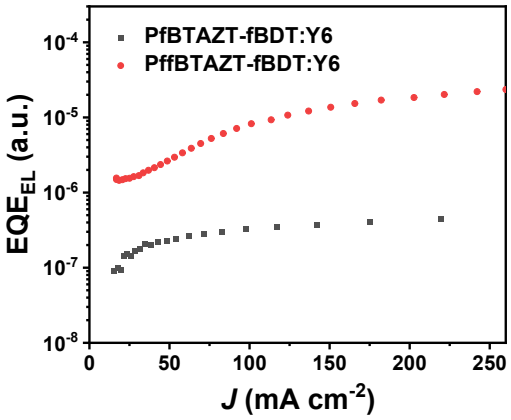

Fig. S8 EQE_{EL} of optimal OSCs based on polymer:Y6 series.

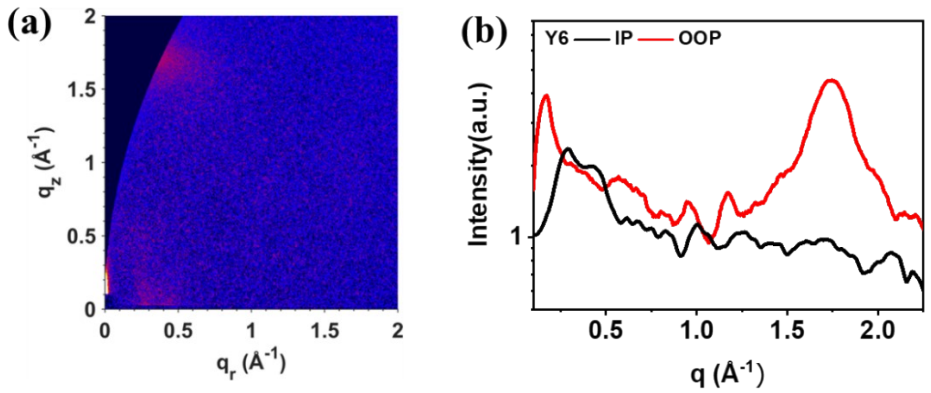

Fig. S9 (a) 2D GIWAXS patterns of pure Y6; (b) The corresponding intensity profiles along the in-plane and out-of-plane directions.

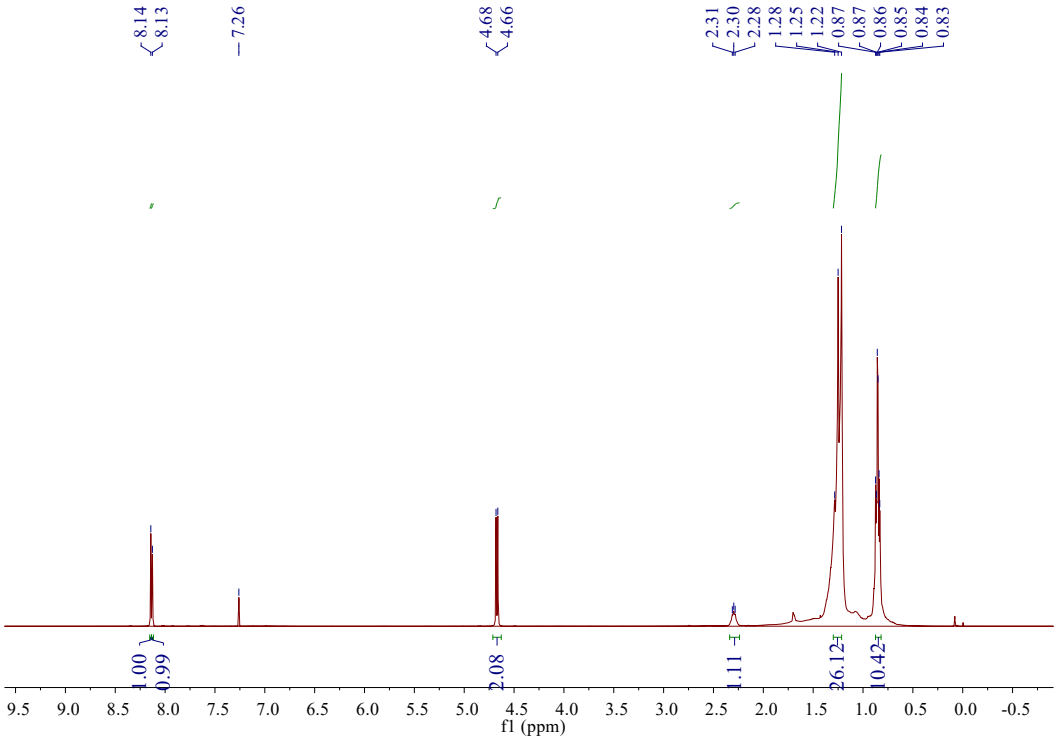

Fig. S10 ^{1}H NMR spectrum of compound 2

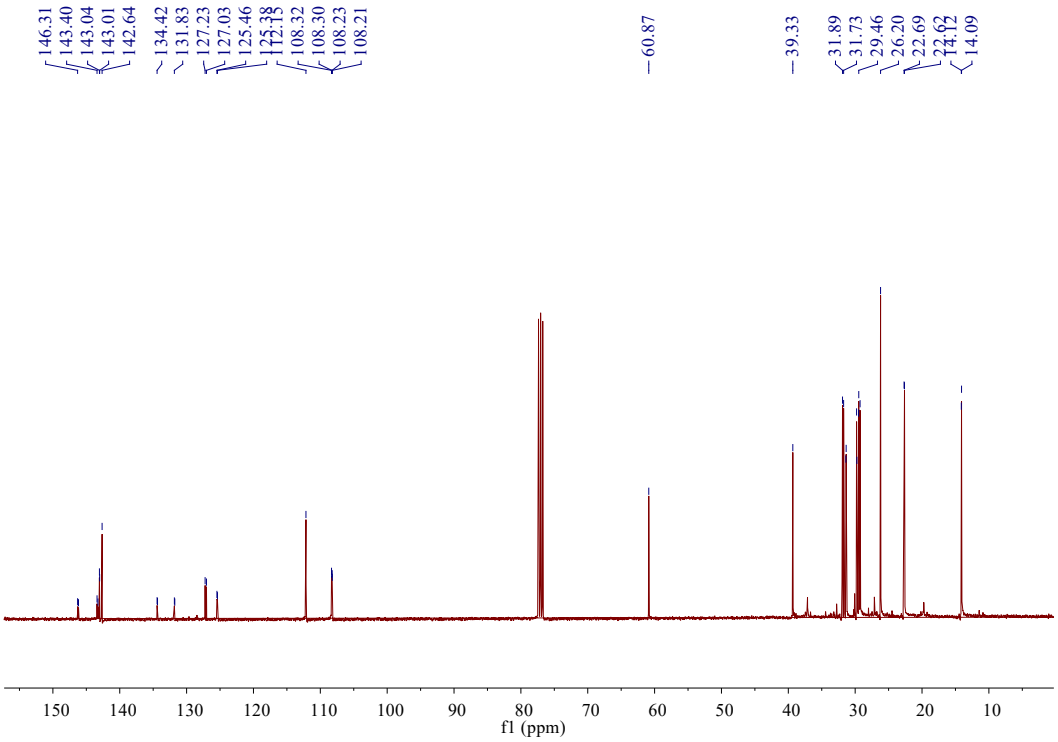

Fig. S11 ^{13}C NMR spectrum of compound 2

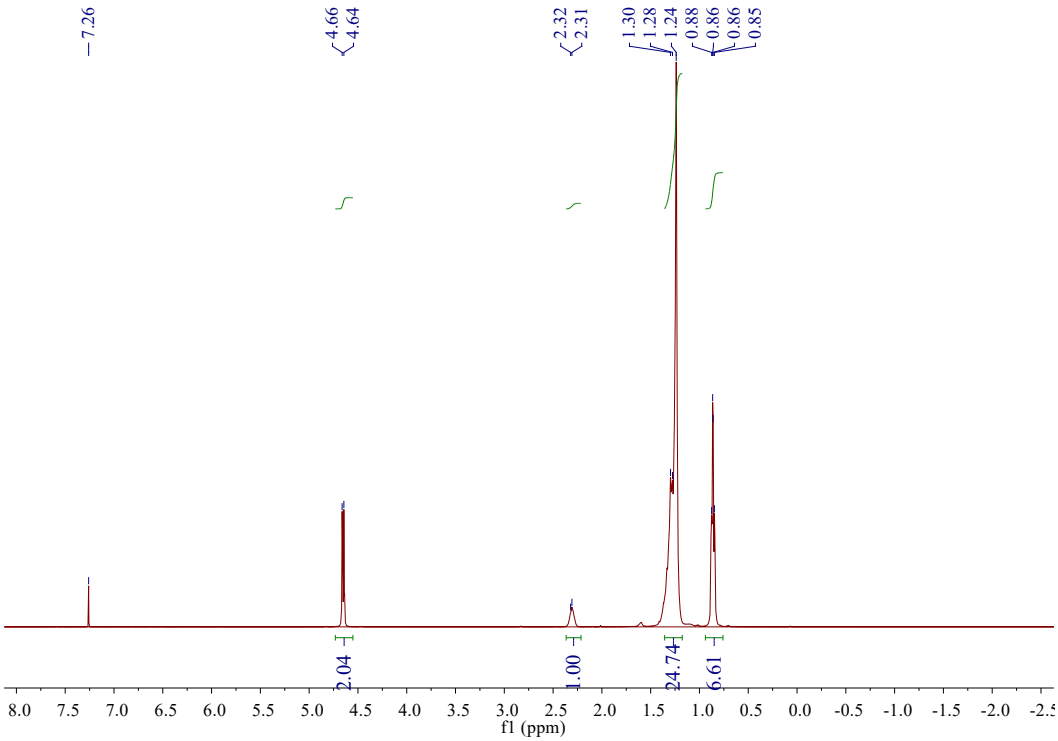

Fig. S12 ^{1}H NMR spectrum of compound 3.

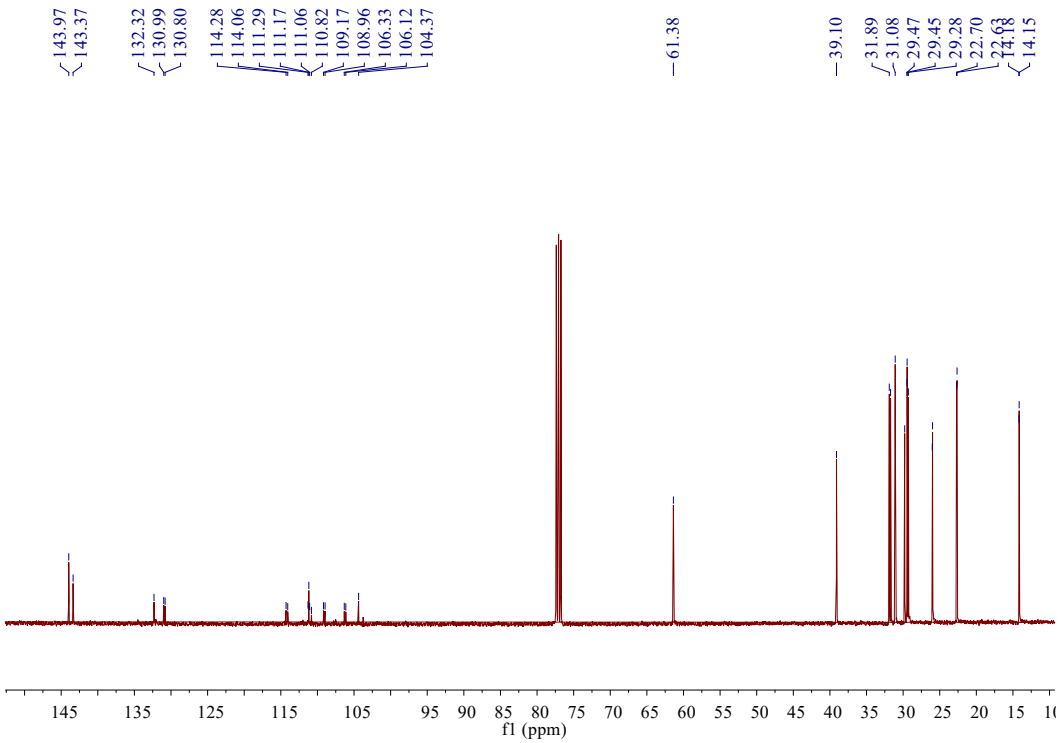

Fig. S13 ^{13}C NMR spectrum of compound 3

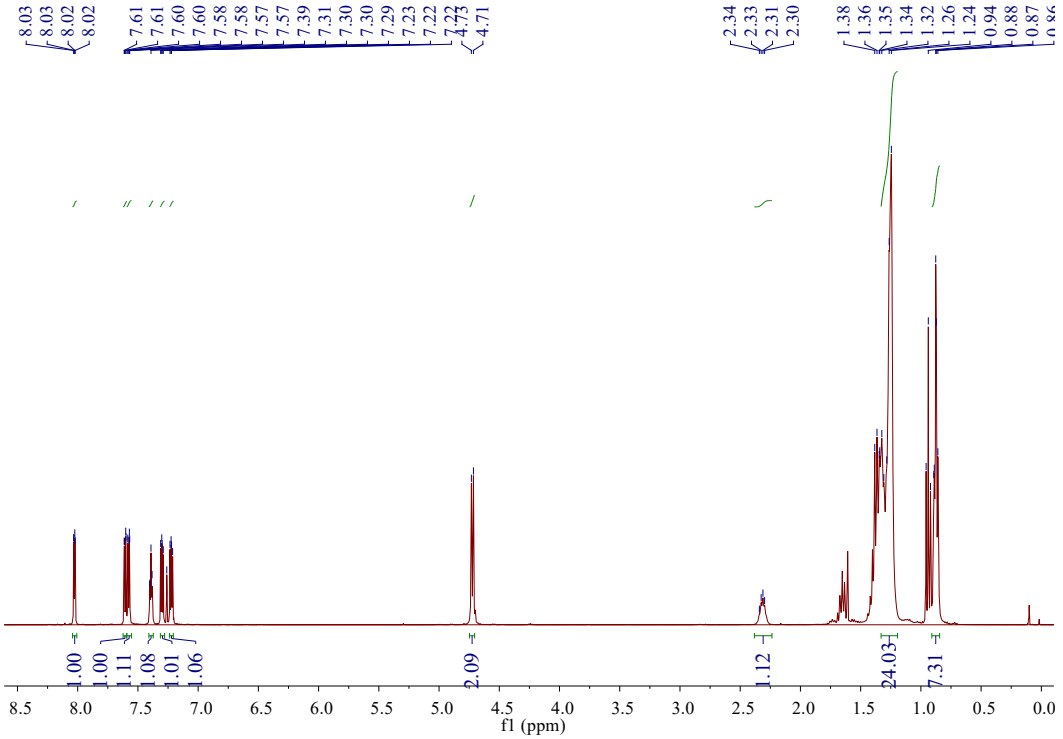

Fig. S14 ^{1}H NMR spectrum of compound 4.

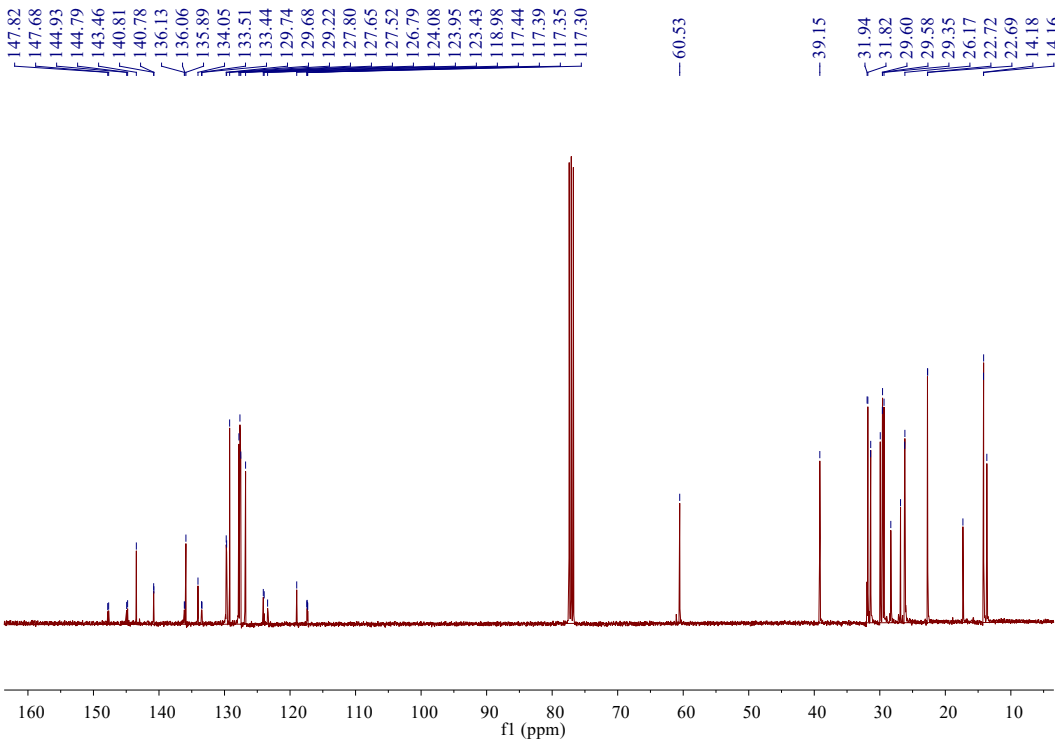

Fig. S15 ^{13}C NMR spectrum of compound 4

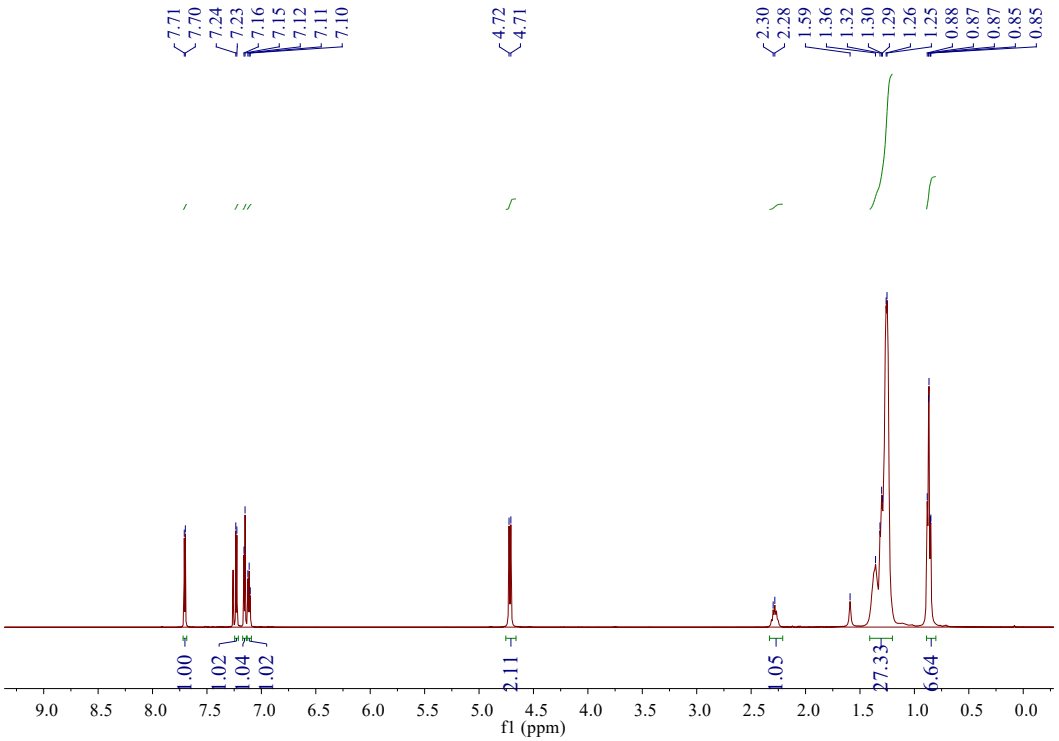

Fig. S16 ^{1}H NMR spectrum of M2.

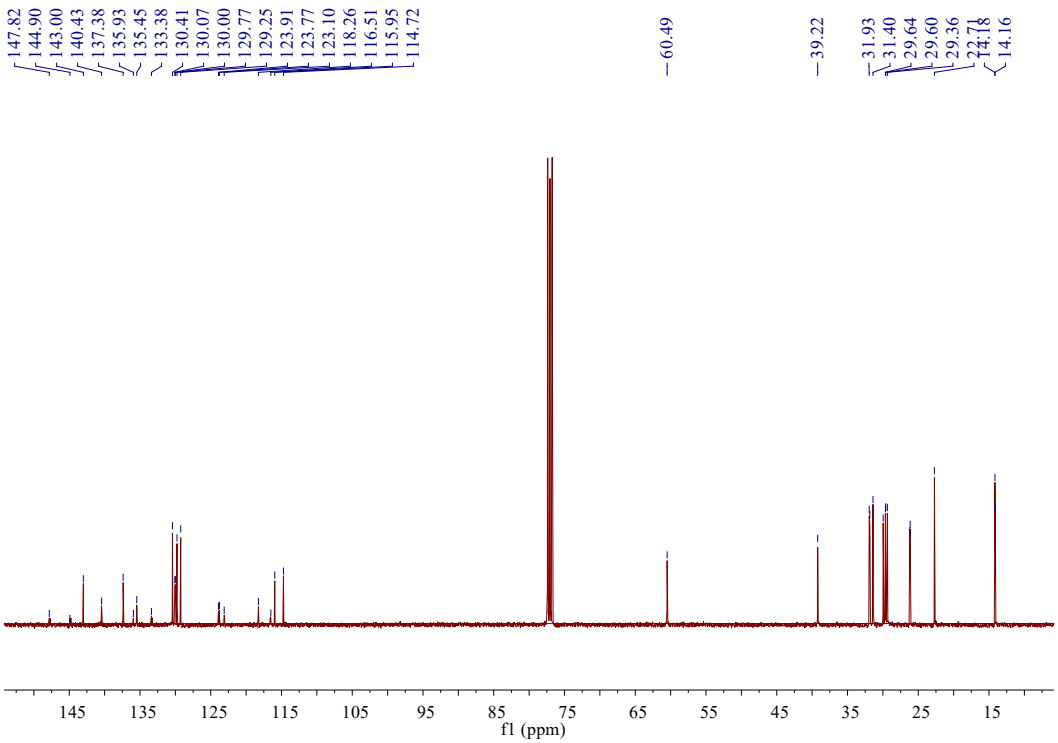

Fig. S17 ^{13}C NMR spectrum of M2

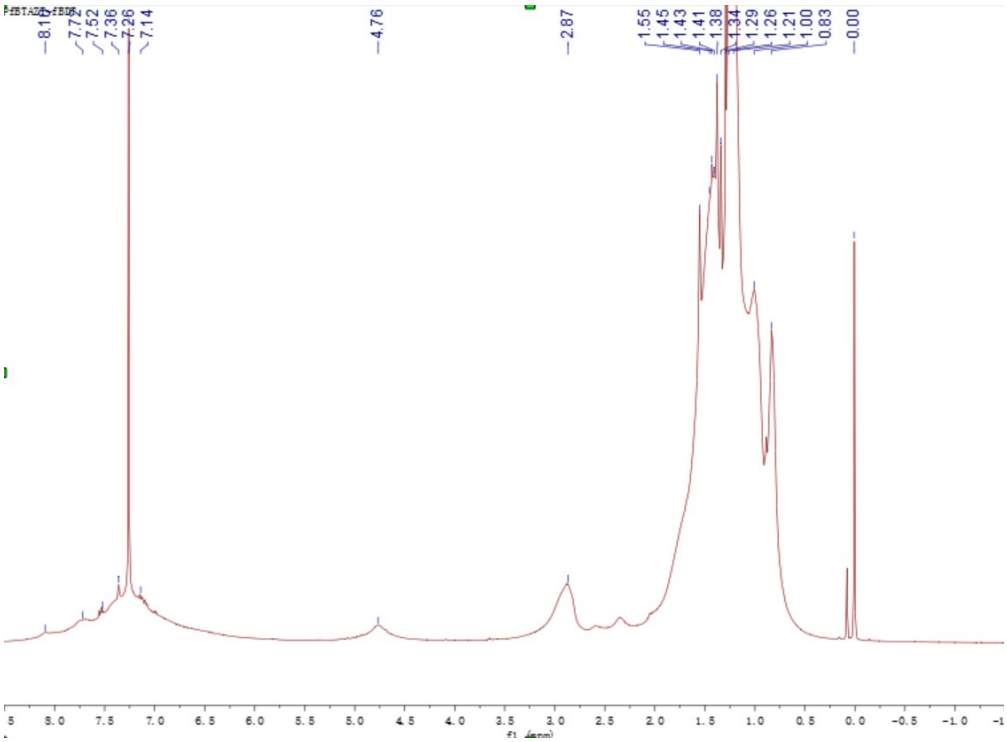

Fig. S18 ^{1}H NMR spectrum of PfBTAZT-fBDT

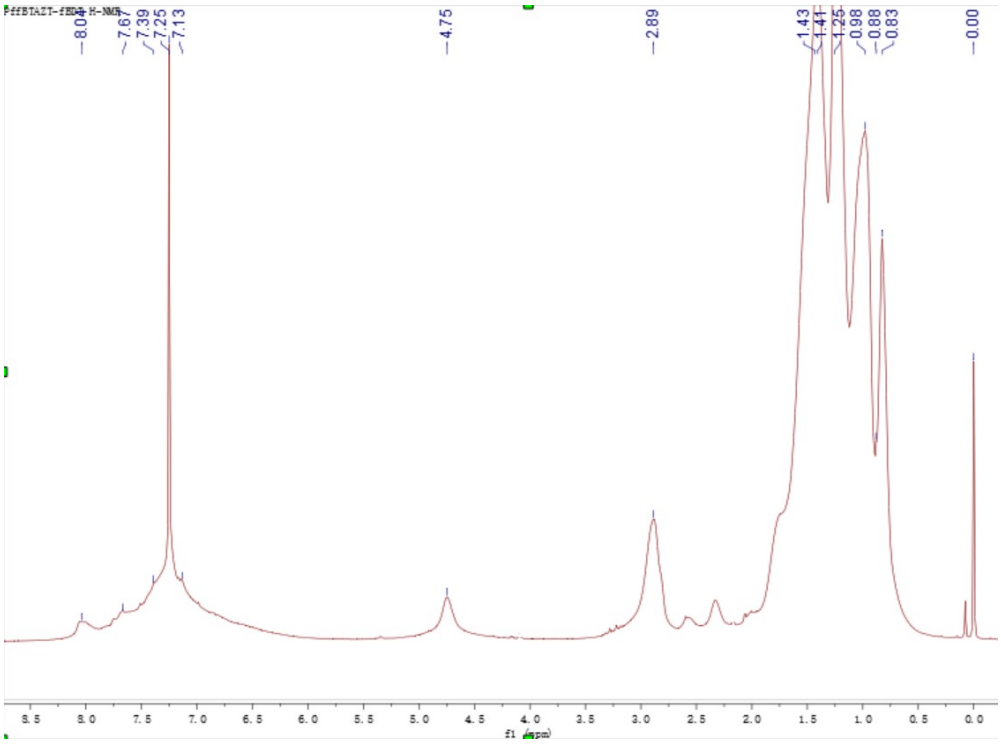

Fig. S19 [1]H NMR spectrum of PffBTAZT-fBDT

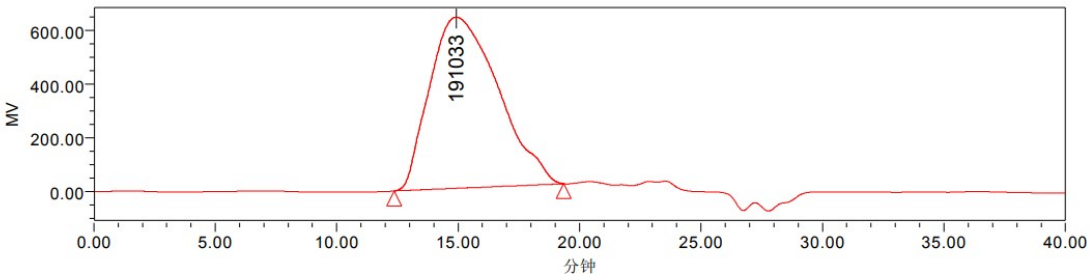

Fig. S20 The GPC curves of **PfBTAZT-fBDT**

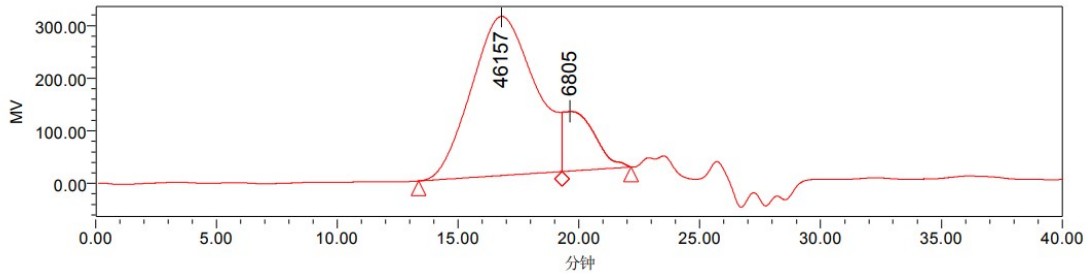

Fig. S21 The GPC curves of **PffBTAZT-fBDT**